Effect of electromagnetically-induced transparency delay generated by dynamic coherent population trapping in Rb vapour

Daba Radnatarov[a], Sergey Khripunov[a], Sergey Kobtsev[a], Alexey Taichenachev[a,b], Valery Yudin[a,b], Maxim Basalaev[a,b], Ivan Popkov[a], Valeriy Andryushkov[a]
[a]Novosibirsk State University, Pirogova str., 2, Novosibirsk, 630090, Russia;
[b]Institute of Laser Physics SB RAS, Ac. Lavrentyev prosp., 13/3, Novosibirsk, 630090, Russia

ABSTRACT

We present a study of the identified for the first time effect of electromagnetically-induced transparency delay in Rb vapours on the atomic clock transition. The effect consists in the presence of a delay in the time of the maximal total transmission of atomic vapour relative to the moment when a two-photon resonance is reached as the frequency difference between two laser fields (FDLF) deviates around the clock transition frequency. It was found out that the delay is higher for higher frequencies of the FDLF modulation and is accompanied by substantial evolution of the width and shape of the coherent population trapping resonance.

Keywords: electromagnetically-induced transparency, coherent population trapping, CPT resonance, atomic clock

1. INTRODUCTION

In recent years, many groups around the world have been actively studying the effect of coherent population trapping (CPT) in alkali metals and the related to it effect of electromagnetically-induced transparency (EIT). The effect of CPT consists in the studied medium atoms falling into the so-called 'dark' resonant state when pumped with a bi-chromatic optical field with the frequency difference close to that of the hyperfine splitting. Atoms occupying this state cease to interact with the optical field, leading to observation of EIT[1]. CPT resonances occurring in alkali metal atoms are known for their high quality factor[2] of ~10^8, thus allowing their application as a quantum discriminator in frequency standards[3-6] and magnetometers[7,8]. For locking in the frequency of a quartz oscillator to the reference CPT resonance, the frequency difference of the bi-chromatic field around the resonance is modulated and a feed-back system with a lock-in amplifier is used. One of the advantages of this method is the possibility of noise filtering in the measurement system at frequencies not immediately adjacent to the modulation frequency[9]. Given the fact that the noise intensity is reduced as the frequency rises, selection of higher modulation frequency leads to lower noise level in the feed-back system, thus improving the device performance. However, higher frequencies introduce a number of effects related to a finite time of excitation and relaxation of the coherent 'dark state'. One of these effects is the maximal value of EIT delayed in time with respect to the moment when the difference frequency of the bi-chromatic field coincides with the resonant one. Since the field frequency difference changes periodically, this temporal delay of the EIT reaching its maximum (or of the CPT resonance transmission maximum) may be treated as a phase delay with relation to the reference signal from the lock-in amplifier. This work is devoted to study of the phase delay in formation of CPT resonance peaks in Rb^{87} atoms.

2. THEORY

Our theoretical treatment of CPT resonance dynamics in Λ-systems (see Fig. 1) pumped with bi-chromatic fields was carried out on the basis of the equations for the atomic density matrix, which take the following form in the resonant approximation

*d.radnatarov@gmail.com; phone/fax +7 383 363 4265; www.nsu.ru/srd/lls/english/index.htm

Slow Light, Fast Light, and Opto-Atomic Precision Metrology IX, edited by Selim M. Shahriar, Jacob Scheuer, Proc. of SPIE Vol. 9763, 97630A · © 2016 SPIE
CCC code: 0277-786X/16/$18 · doi: 10.1117/12.2209470

$$
\begin{aligned}
&\frac{\partial \rho_{21}}{\partial t} = -\left[\Gamma_0 + i(\delta_2 - \delta_1)\right]\rho_{21} - i\Omega_1\rho_{23} - i\Omega_2^*\rho_{31},\\
&\frac{\partial \rho_{31}}{\partial t} = -(\gamma_{opt} - i\delta_1)\rho_{31} - i\Omega_1(\rho_{11} - \rho_{33}) + i\Omega_2\rho_{21},\\
&\frac{\partial \rho_{32}}{\partial t} = -(\gamma_{opt} - i\delta_2)\rho_{32} + i\Omega_2(\rho_{22} - \rho_{33}) + i\Omega_1\rho_{12},\\
&\frac{\partial \rho_{11}}{\partial t} = \frac{\gamma_{sp}}{2}\rho_{33} + \frac{\Gamma_0}{2}\mathrm{Tr}[\hat{\rho}] - \Gamma_0\rho_{11} - i\Omega_1\rho_{13} + i\Omega_1^*\rho_{31}, \qquad (1)\\
&\frac{\partial \rho_{22}}{\partial t} = \frac{\gamma_{sp}}{2}\rho_{33} + \frac{\Gamma_0}{2}\mathrm{Tr}[\hat{\rho}] - \Gamma_0\rho_{22} - i\Omega_2\rho_{23} + i\Omega_2^*\rho_{32},\\
&\frac{\partial \rho_{33}}{\partial t} = -(\gamma_{sp} + \Gamma_0)\rho_{33} + i\Omega_1\rho_{13} + i\Omega_2\rho_{23} - i\Omega_1^*\rho_{31} - i\Omega_2^*\rho_{32},\\
&\rho_{12} = \rho_{21}^*, \quad \rho_{13} = \rho_{31}^*, \quad \rho_{23} = \rho_{32}^*,\\
&\mathrm{Tr}[\hat{\rho}] = \rho_{11} + \rho_{22} + \rho_{33} = 1,
\end{aligned}
$$

where $\Omega_{1,2}$ are the Rabi frequencies; γ_{sp} is the decay rate of the excited level $|3\rangle$; γ_{opt} is the total decoherence rate (spontaneous, collision, time-of-flight) of the optical transitions $|1\rangle \to |3\rangle$ and $|2\rangle \to |3\rangle$; Γ_0 is the relaxation rate of the lower energy levels to the equilibrium isotropic state: $\left(|1\rangle\langle 1| + |2\rangle\langle 2|\right)/2$; $\delta_k = \omega_k - \omega_{3k}$ $(k = 1,2)$ is the detuning of the *k*-th field frequency from the frequency of the respective resonant transition. Simultaneous equations (1) were solved by the method fully explained in our work [10], which allows to calculate the periodical steady state without solving the full problem with initial conditions and without Fourier decomposition.

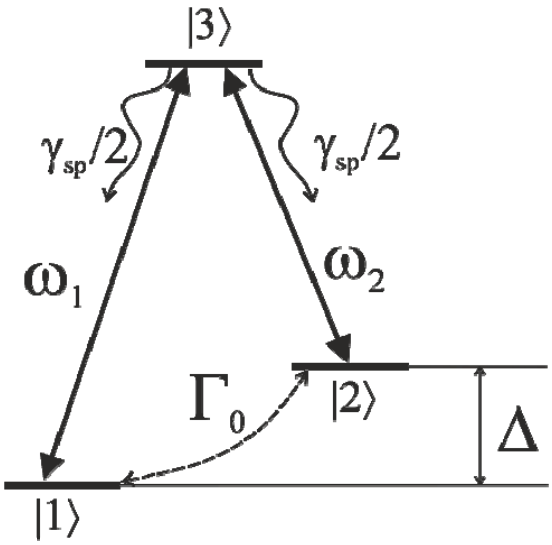

Fig. 1. Three-level Λ-system in a bi-chromatic field.

In Fig. 2, the calculated dependencies of the intensity of the radiation passed through a rubidium vapour cell are given for different frequencies of harmonic excitation of the CPT resonance. In order to compare in the same plot the shapes of resonant curves corresponding to several modulation frequencies (which may differ from one another by as much as two

orders of magnitude) the horizontal axis is chosen to show the modulation signal phase at different modulation frequencies. It can be seen from Fig. 2 that the CPT resonance shape undergoes material changes when the excitation frequency is swept from 4 to 400 Hz. Anharmonic oscillations emerge in its trailing wing as a consequence of beating between populations of the excited state[11]. The central part of the CPT resonance is also transformed: as the frequency rises, it broadens, its magnitude drops, and the phase position of its peak is shifted. At low modulation frequencies (several Hz), the resonance shape has a Lorentzian shape, which corresponds to the stationary case[12].

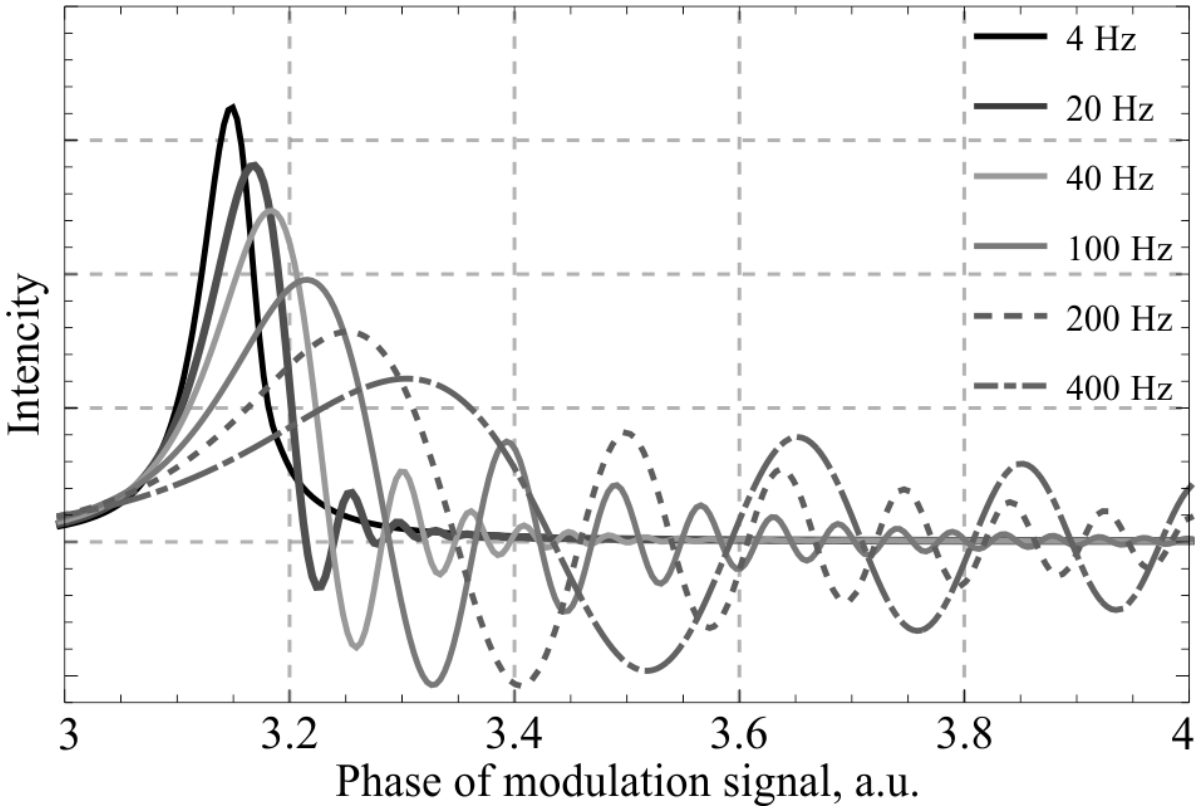

Fig. 2. Calculated dependencies of the intensity of radiation at the exit from the vapour cell upon the modulation signal phase at different modulation frequencies.

3. EXPERIMENT

Our experimental studies of the phase delay of CPT resonance formation were conducted on the installation schematically depicted in Fig. 3. The injection current of a single-frequency vertical-cavity semiconductor laser pump was modulated at the frequency of 3.417 GHz generated with a frequency synthesiser Phase Matrix 10 GHz. This led to emergence of two side components in the laser radiation spectrum detuned from the central peak by ± 3.417 GHz. A 10-MHz reference signal was provided by a rubidium atomic clock with relative instability of 10^{-12}/t. The frequency difference between the side components of the laser radiation corresponded to the frequency of the transition between the levels of hyperfine splitting of the fundamental state of ^{87}Rb. To create a CPT resonance, the frequency difference between the side modes was modulated at a frequency that could be adjusted in the range of 0.1–5,000 Hz, the modulation amplitude remaining constant at 1 kHz. The pumping radiation was then guided into a spherical optical cell having a diameter of 13 mm, anti-relaxation coating of the internal walls, and filled with ^{87}Rb vapour. The intensity of the laser radiation passed through the cell was registered by a photo-detector with a 100-kHz bandwidth. In order to eliminate any external magnetic field, the optical cell was placed inside a three-layer magnetic shield. Both the pump laser and the optical cell were thermo-stabilised and their temperature instability did not exceed 10^{-3} °C. The power of the laser radiation entering the optical cell was 50 uW.

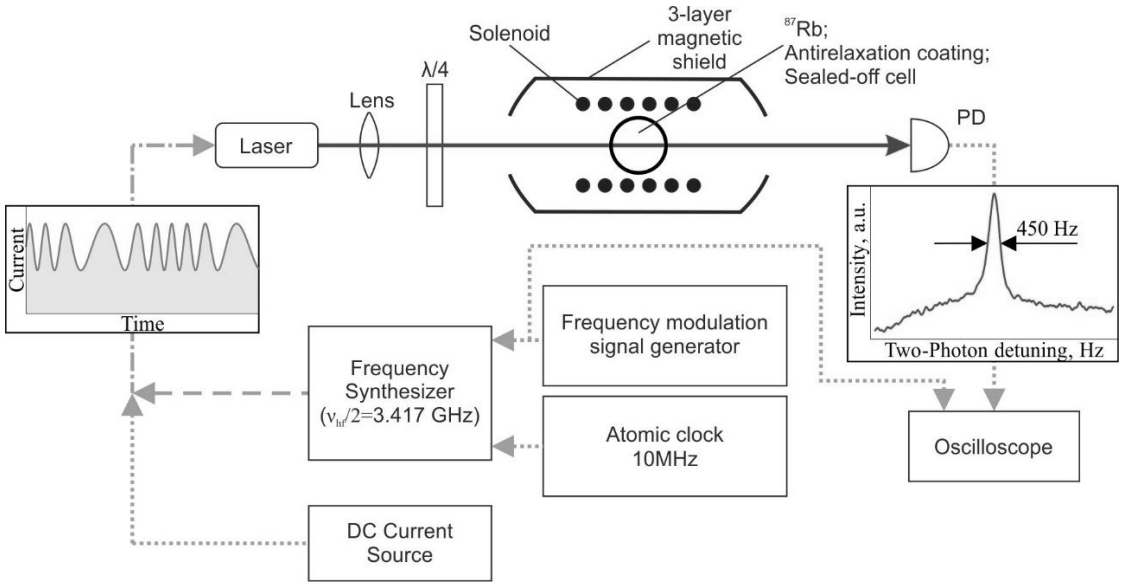

Fig. 3. Diagram of the experimental installation.

At relatively slow modulation rates of the RF signal frequency, an almost Lorentzian 450-Hz-wide CPT resonance was observed (Fig. 3). As the modulation frequency was augmented, the shape of the resonant curve also evolved (Fig. 4): the peak grew lower and broader and anharmonic oscillations appeared in the trailing wing of the resonant curve. The evolution of the resonant curve shape correlated with the theoretical curves presented in Fig. 2. As it can be seen in Fig. 4, at higher modulation frequencies, the resonant curve peak shifted to the right, which means that it was formed after a delay with respect to the moment when the frequency difference of the bi-chromatic field was exactly equal to that of the hyperfine splitting.

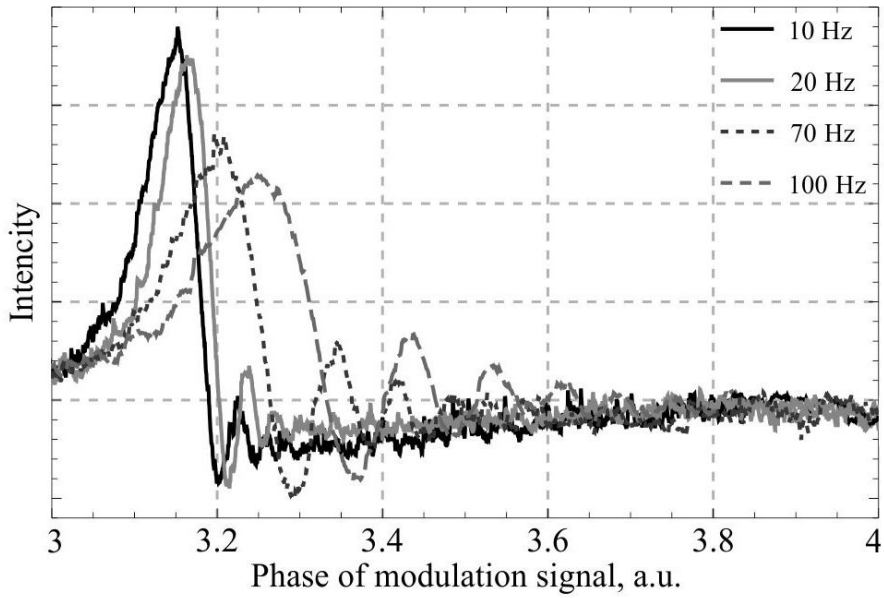

Fig. 4. Experimentally measured dependence of the intensity of the radiation exiting the vapour cell upon the modulation signal phase at different modulation frequencies, modulation amplitude being 1 kHz.

Both measured and theoretical dependencies of the amount of phase delay of the peak position of the resonant curve upon the modulation frequency at a constant modulation amplitude are presented in Fig. 5. The presented graph demonstrates that at low modulation frequencies not exceeding 1.8 kHz, the amount of phase delay is directly proportional to the modulation frequency with the proportionality coefficient of 1.1×10^{-3} rad/Hz. In the temporal representation, since the modulation period is inversely proportional to the frequency, this direct proportionality of the phase delay corresponds to the presence of a constant (independent of the frequency) delay of the establishment of the maximal EIT (or the maximum of the CPT resonance transmission) equal to 0.17 ms. As the modulation frequency was increased from 1.8 to 4.5 kHz, the phase delay of the CPT resonance maximum grew much slower and did not exceed 2.2 rad, corresponding to reduced delay in the temporal representation.

In order to ascertain that the phase delay registered in the experiment was not an effect of the measurement apparatus, we measured the phase delays arising in modulation of the RF signal. This was done by feeding the signal from the frequency synthesiser into a real-time RF spectrum analyser with demodulation capability Tektronix 3308B, triggered by the modulation signal. Our measurements have shown that the synthesiser phase delay at low frequencies (below 100 Hz) did not exceed 0.5 rad and quickly dropped at higher frequencies. This hardware phase delay was taken into account in Fig. 5.

Numerical modelling of the dependence of the phase delay upon the modulation frequency revealed a qualitatively similar behaviour: at low modulation frequency, the phase delay depended on it linearly, but as the frequency was increased, the phase delay slowly grew and approached the value of $\pi/2$, which was then exceeded at frequencies higher than 10 kHz.

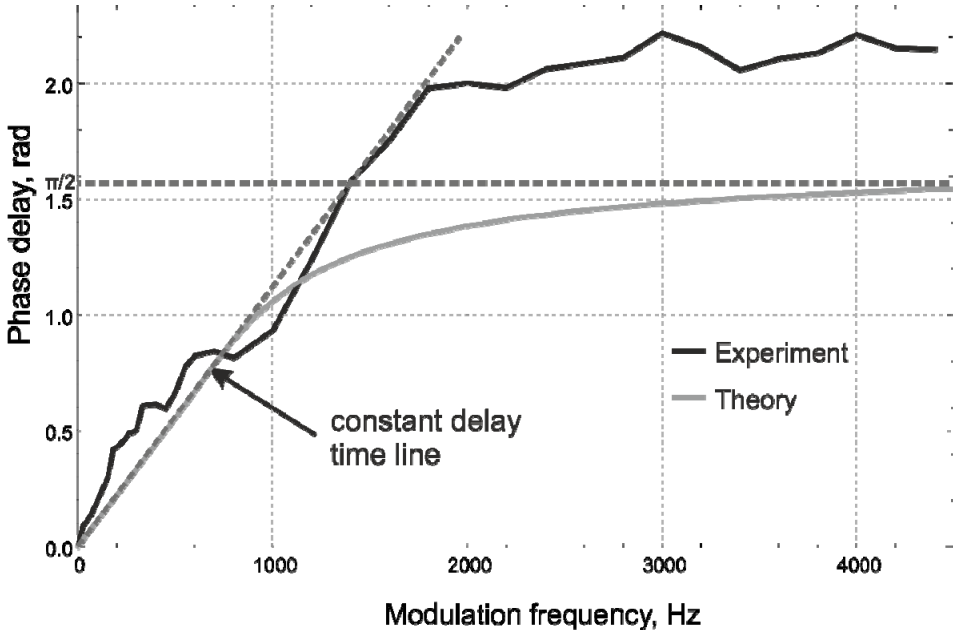

Fig. 5. The experimental and theoretical dependencies of the phase delay of the cell transmission peak upon the modulation frequency of the frequency difference of the bi-chromatic field at the constant modulation amplitude of 1 kHz.

CONCLUSION

The conducted research for the first time uncovered the presence of a temporal delay of the moment of the maximal electromagnetically-induced transparency relative to the moment when the frequency difference of the bi-chromatic field equals the resonant one, the delay value amounting to 0.17 ms. When the CPT resonance is periodically excited by a bi-chromatic field with modulated frequency difference, this delay may be treated as a phase delay, whose value depends

linearly on the modulation frequency between 0 and ~1.8 kHz. As the modulation frequency is further raised, the phase delay growth gets gradually saturated, the experimental and theoretical saturation values differing by ~0.6 rad. Perhaps, this discrepancy is created by other measurement apparatus delays other than that introduced by the frequency synthesiser. It is also possible that the chosen theoretical model is incomplete.

The existence of a phase delay itself does not directly affect the feed-back system comprising a lock-in amplifier because lock-in amplifiers usually contain built-in adjustable delay lines for shifting the reference signal. These delay lines are included for compensation of phase delays introduced by electronic components of the feed-back system and may be equally used for compensation of the newly identified temporal delay in formation of CPT resonances.

Continued study of the effect of phase delay of CPT resonance formation is essential since this effect is closely related to the process and mechanisms of the CPT resonance formation. The dependence of this phase delay upon the modulation frequency characterises velocities of the processes of excitation and relaxation of the 'dark' atomic states.

ACKNOWLEDGMENTS

This work was supported by the Grants of Ministry of Education and Science of the Russian Federation (agreement No. 14.B25.31.0003, ZN-06-14/2419, order No. 3.162.2014/K, 2014/139, 825); Grants of the Russian Foundation of Basic Research (No. 16-32-60050, 16-32-00127, 16-32-60160, 16-32-00899, 16-32-00781).

REFERENCES

[1] Alzetta, G., Gozzini, A., Moi, L. and Orriols, G., "An experimental method for the observation of r.f. transitions and laser beat resonances in oriented Na vapour", Il Nuovo Cimento B Series 11, 36(1), 5–20. (1976)
[2] Vanier, J., "Coherent population trapping for the realization of a small, stable, atomic clock", Frequency Control Symposium and PDA Exhibition, 2002. IEEE International (2002)
[3] Zhong, W., "Review of chip-scale atomic clocks based on coherent population trapping", Chin.Phys.B 23(3), 030601 (2014).
[4] Masian, Y., Sivak, A., Sevostianov, D., Vassiliev, V. and Velichansky, V., "Study and optimization of CPT resonance parameters in ^{87}Rb/Ar/Ne microcells aimed for application in metrology", Physics Procedia 71, 252-256 (2015).
[5] Vanier, J. and Tomescu, C., "The quantum physics of atomic frequency standards: recent developments", CRC Press, 486p., 2015, ISBN 9781466576957.
[6] Khripunov, S., Radnatarov, D. and Kobtsev, S., "Atomic clock based on a coherent population trapping resonance in 87 Rb with improved high-frequency modulation parameters", Proc. SPIE 9378, 93780A (2015).
[7] Schwindt, P. D., Knappe, S., Shah, V., Hollberg, L., Kitching, J., Liew, L. A. and Moreland, J., "Chip-scale atomic magnetometer", Appl. Phys. Lett. 85(26), 6409–6411 (2004).
[8] Shah, V. K. and Wakai, R. T., "A compact, high performance atomic magnetometer for biomedical applications", Physics in Medicine and Biology 58, 8153 (2013).
[9] Meade, M. L., "Lock-in amplifiers: principles and applications", Peter Peregrinus Ltd., 232p., 1983, ISBN 9780906048948.
[10] Yudin, V. I., Taichenachev, A. V. and Basalaev, M. Y., "Dynamic steady-state of periodically-driven quantum systems", Phys. Rev. A 93, 013820 (2016).
[11] Wang, Z., Zhao, J., Zhao, X., Liu, L., Zhuang, Y. and Li, D., "An atomic frequency micrometer based on the coherent population beating phenomenon", Jt. Conf. IEEE Int., 465–470 (2015).
[12] Knappe, S., Hollberg, L. and Kitching, J., "Dark-line atomic resonances in submillimeter structures", Opt. Lett. 29(4), 388–390 (2004).